High-throughput quantitation of intracellular trafficking and organelle disruption by flow cytometry

Pei Zhi Cheryl Chia, Yasmin M. Ramdzan, Fiona J. Houghton, Danny M. Hatters and Paul A. Gleeson

The Department of Biochemistry and Molecular Biology and Bio21 Molecular Science and Biotechnology Institute, The University of Melbourne, Victoria 3010, Australia

[1]**Corresponding author:** Prof. Paul Gleeson**,** Department of Biochemistry and Molecular Biology and Bio21 Molecular Science and Biotechnology Institute**,** The University of Melbourne**,**Victoria 3010**,** Australia**,** Phone 61-3-8344-2354:Fax 61-3-9348-1428, E-mail: pgleeson@unimelb.edu.au

Abbreviations: PulSA, pulse shape analysis, Wls, Wntless; TGN, trans-Golgi network; STxB, Shiga toxin B subunit, siRNA, small interfering RNA

synopsis

Standard approaches for analysing the intracellular location of membrane cargo involves microscopy-based methods, which have limitations in throughput capacity and acquisition speed. We describe a flow cytometry based-method, which allows 1000s of cells to be analysed per second. We demonstrate that fluorescence pulse-width, a standard parameter of flow cytometers, can be used to determine the location of membrane proteins, to monitor their trafficking and can be exploited to sort cells based on differences in the intracellular localisation of membrane proteins.

Abstract

Current methods for the quantitation of membrane protein trafficking rely heavily on microscopy, which has limited quantitative capacity for analyses of cell populations and is cumbersome to perform. Here we describe a simple flow cytometry-based method that circumvents these limitations. The method utilizes fluorescent pulse-width measurements as a highly sensitive indicator to monitor the changes in intracellular distributions of a fluorescently labelled molecule in a cell. Pulse-width analysis enabled us to discriminate cells with target proteins in different intracellular locations including Golgi, lyso-endosomal network and the plasma membrane, as well as detecting morphological changes in organelles such as Golgi perturbation. The movement of endogenous and exogenous retrograde cargo was tracked from plasma membranes-to-endosomes-to-Golgi, by decreasing pulse-width values. A block in transport upon RNAi-mediated ablation of transport machinery was readily quantified, demonstrating the versatility of this technique to identify pathway inhibitors. We also showed that pulse-width can be exploited to sort and recover cells based on different intracellular staining patterns, for example early endosomes and Golgi, opening up novel downstream applications. Overall, the method provides new capabilities for viewing membrane transport in thousands of cells per minute, unbiased analysis of the trafficking of cargo, and the potential for rapid screening of inhibitors of trafficking pathways.

Keywords: fluorescence pulse-shape, intracellular location, Golgi, membrane transport, retrograde transport, flow cytometry

This article has been accepted for publication and undergone full peer review but has not been through the copyediting, typesetting, pagination and proofreading process, which may lead to differences between this version and the Version of Record. Please cite this article as doi: 10.1111/tra.12161

Introduction

Knowledge of the intracellular location of membrane proteins is critical in defining functional roles. Many membrane proteins recycle between two or more intracellular compartments and regulated trafficking is central to their function (1). Standard approaches for analysing the intracellular location of cargo involves microscopy-based methods that have limitations in their throughput capacity, speed of acquisition and quantitation. The development of fast, sensitive and quantitative approaches to detect intracellular localization and trafficking would represent a significant advance in the field. In contrast to microscopy, flow cytometry has the capacity to analyze thousands of cells per second. We have recently described pulse shape analysis (PulSA), the measurement of the pulse-width and height of a fluorescently labelled molecule, to monitor protein localization in cells by flow cytometry (2). For example we showed that PulSA could monitor protein aggregation, cytoplasmic to nuclear translocation and discrimination between plasma membrane and Golgi location. The classical use of flow cytometry has involved collection of the total fluorescence emitted by each cell, eg pulse area, as it passes through the laser light beam, rather than using the instrument to quantitate different intracellular locations. Flow cytometry analyses are usually represented as pulse areas. However, pulse-width is an available parameter that provides information about the size of the fluorescent structure or particle. Pulse-width has been used to discriminate a pulse due to a single cell from a pulse from a doublet (two cells stuck together) (3) and also to monitor nuclear size of cells (4). PulSA and pulse-width have considerable potential for other applications. A most promising, but thus far unheralded, application is in monitoring trafficking of cargo between intracellular compartments within a large cell population or in monitoring abnormal distributions of particular organelles throughout the cytoplasm. The current use of microscopy for quantitation of membrane transport requires many hours for image collection to obtain data of only a relatively small number of cells (typically 50-100 cells) followed by labour intensive image analysis. Furthermore, an inherent problem with microscopic analysis is the potential bias in the selection of a limited number of cells in the population for analysis. Here we explored the use of PulSA to circumvent these problems and demonstrate that pulse-width can be used to rapidly monitor intracellular endosome-to-Golgi transport processes of the entire cell population very rapidly. In addition, we demonstrate the application of PulSA to monitor alterations in the morphology of the Golgi arising from drug treatment and for sorting of cells based on intracellular location of membrane proteins. The application of flow cytometry provides a considerable advance in speed of quantitative analysis of these intracellular processes in cell populations.

Results

Use of flow cytometry to distinguish membrane cargo at the cell surface and the Golgi apparatus

We have recently described pulse-shape analysis (PulSA) (Fig. 1A) to discriminate differences in protein localization in cells by flow cytometry (2). This earlier study demonstrated it was possible to distinguish between cells with proteins at the cell surface from proteins within the Golgi, however, it was unclear if PulSA could be used to analyse the steady state localisation of membrane proteins that are continually recycling or to monitor dynamic processes associated with trafficking. To investigate these possibilities, firstly we determined whether the differences in location between a wild-type and mutant membrane protein could be distinguished by PulSA. For this analysis we analysed the multi-pass membrane protein Wntless (Wls), which is a specific cargo receptor for delivery of Wnt signalling proteins from the *trans*-Golgi network (TGN) to the cell surface (5). Wls continuously recycles between the cell surface and the TGN and under steady-state conditions the majority of Wls is located at the TGN. We have described an endocytosis-defective Wls mutant, a YEGL sequence in the 3rd intracellular loop mutated to AEGL, which accumulates at the cell surface (6). To determine if PulSA could discriminate between the intracellular distributions of wild-type and mutant Wls, HeLa cells were transfected with HA-tagged Wls constructs, cells harvested by incubation with EDTA/PBS and stained in suspension using an antibody which recognises a cytoplasmically-orientated HA tag, and labelled cells analysed by immunofluorescence and by flow cytometry. As expected, immunofluorescence of suspension cells revealed that hWls^{AEGL} showed a marked difference in location compared with hWls^{wt} (Fig. 1B). hWls^{AEGL} was localised predominantly at the cell surface, confirming a block in internalisation, whereas the majority of hWls^{wt} was localised in the Golgi region as indicated by the co-localisation with the Golgi marker, GRASP65. We analysed the stained cell populations by PulSA with over 10,000 events collected. A clear difference in pulse-width distributions was observed between hWls^{wt} and hWls^{AEGL} expressing cells (Fig. 1C). The pulse-width of cells expressing hWls^{AEGL} was considerable broader than the population expressing hWls^{wt}. Fig. 1C shows the data overlaid from three independent experiments. The thickness of the histogram curve reflects the level of consistency of data across the three experiments. The three independent experiments showed a high level of co-incidence. The median pulse-width of hWls^{wt} expressing cells is significantly different from the median of cells expressing hWls^{AEGL}. Hence pulse-width can readily detect alterations in steady state distribution of mutant membrane proteins.

Use of flow cytometry to monitor cargo trafficking from the cell surface and the Golgi apparatus

Given the finding that a plasma membrane (PM) and Golgi location for membrane proteins could be readily distinguished by flow cytometry, we next assessed the capacity of PulSA to monitor the kinetics of cargo movement from the cell surface to the Golgi. The general procedure is illustrated in the flowchart of Fig. 2. Shiga toxin has been extensively used as a cargo that is transported from the PM to the Golgi via endosomes (7). Previously we showed that PM localised Shiga toxin could be distinguished from Golgi localised Shiga toxin by PulSA (2). Here we have investigated the kinetics of the dynamic

transport process in more detail and analysed the internalisation and trafficking of Cy3 labelled-Shiga toxin B subunit (Cy3-STxB) from the PM over a 60 min period at 37°C. For Shiga toxin trafficking experiments we found that PM-to-Golgi transport was more efficient in cell monolayers than cells in suspension, therefore Shiga toxin trafficking experiments were carried out on monolayers prior to cell harvesting, as described in Materials and Methods, whereas for other cargos the transport assays were performed in cell suspensions. The PulSA data for the 0, 15 and 30 min time points of Cy3-STxB transport are shown in Fig. 3A. Each time-point shows the merger of 3 independent experiments. A high level of reproducibility was observed. By 15 min incubation at 37°C the population of cells showed a shift in pulse-width with a smaller pulse-width than the population at 0 min. Extending the incubation from 15 min resulted in a smaller additional shift. The pulse-width of GM130 as a Golgi marker remained constant during the incubation period (Fig. 3A). Moreover, the intracellular location of the Cy3-STxB as assessed by microscopy was consistent with the flow cytometry data; by 15 min internalisation cells showed a juxtanuclear staining pattern which overlapped with GM130 (Fig. 3B). These PulSA data show that the cells in the population behave uniformly with similar kinetics of PM-to-Golgi transport of STxB throughout the whole population.

Furin is a membrane protein which recycles between the PM and Golgi via the late endosomes (8, 9). We also examined the transport of Flag-furin, from the PM to the Golgi in transfected HeLa cells in cell suspension, using an anti-Flag antibody internalisation assay (9). The monolayers were lifted with EDTA/PBS rather than trypsinization to avoid loss of surface Flag-furin molecules. Analysis of the trafficking of Flag-furin by immunofluorescence showed that furin is transported from the PM to the Golgi over a 60 min period (Fig. S1A), kinetics of furin transport similar to that previously reported for adherent HeLa cells (9). At 15 min internalisation at 37°C Flag-furin was detected as punctate structures in the cytoplasm by microscopy and at 60 min there was substantial co-localisation of Flag-furin with the Golgi marker, GM130 (Fig. S1A). FACS PulSA analysis of the population at each time point allowed the Flag-furin-positive HeLa cells to be distinguished from non-transfected cells and analysis of the fluorescence of the antibody-Flag-furin complex by PulSA showed shifts to smaller pulse-widths at 15 min and at 60 min time points, with a pulse-width at 60 min overlapping the Golgi marker GM130 (Fig. S1). A 90 min internalisation showed the same pulse-width as the 60 min time point. Hence the use of PulSA allows the analysis of heterogeneous populations of transiently transfected cells and is applicable to different cargo with different retrograde trafficking routes.

Perturbations of cargo trafficking and organelle morphology by RNAi and drugs can be analysed in cell populations by PulSA

A common approach to define the specific machinery that regulates cargo transport is the use of RNAi and assessment of cargo trafficking by immunofluorescence. Assessment of the entire population by PulSA would provide greatly enhanced quantitative capacity compared with microscopic analysis. We determined if PulSA could be employed to analyse perturbation in the intracellular trafficking of cargo of cell populations using RNAi of machinery components. The cation-dependent mannose 6-phosphate receptor (CI-MPR) recycles between the TGN and endosomes and a perturbation in retrograde trafficking results in a block in this intracellular recycling and the dispersal of MPR into endosomal structures (10). The effect of silencing of machinery on trafficking and localisation ofMPR has typically been assessed by a qualitative approach by scoring the dispersed staining pattern of MPR in a limited number of cells. The recycling of MPR from late endosomes to TGN is Rab9-dependent (11-13) and here we have analysed the intracellular distribution of M6P in Rab9-depleted cells by PulSA. Knock-down of Rab9 was efficient as assessed by Rab9 staining and by flow cytometry; there was a >90% reduction in staining intensity, as assessed by FACS, and only low level staining was observed by confocal microscopy (Fig. 4A). Staining of CI-MPR and analysis by PulSA showed a substantial broadening of the pulse-width in the cell population upon Rab9 knock-down (Fig. 3B). The difference in pulse-width between the control and Rab9 depletion populations was highly significant and very reproducible. The increase in pulse-width following Rab9 knock-down is consistent with the accumulation of CI-MPR in dispersed punctate endosomal structures (Fig. 4B) and demonstrates that PulSA can be effectively used to analyse the intracellular trafficking of a cargo between endosomes and the Golgi within the entire population.

The ability to detect changes not only in intracellular cargo transport but also in organelle location/structure within cells of a population would provide a more quantitative approach to analyze the impact of drugs on organelle morphology compared with the common light microscopic approaches. Various agents including inhibitors of the regulators of Golgi trafficking influence Golgi morphology and result in fragmentation of the Golgi ribbon and dispersal of Golgi membranes throughout the cytoplasm. To determine whether we could use PulSA as a quantitative tool for analysis of Golgi fragmentation, HeLa cells in suspension were treated with brefeldin A (BFA), an inhibitor of Arf1 activation (14), and analysed by PulSA and confocal microscopy. Treatment of HeLa cells with 2 ug/ml of BFA showed the typical change in Golgi staining pattern from a juxtanuclear compact staining pattern to one which showed a dispersed punctate pattern (Fig. 4C). PulSA showed a substantive and reproducible increase in pulse-width of the BFA-treated population of cells compared with the control population, reflecting an increase in the pulse-width of the Golgi marker, GM130. The increase in pulse-width reflects the change from a tight juxtanuclear staining pattern to one which is dispersed throughout the cytoplasm. Moreover, the PulSA data indicates that the majority of cells in a large population are sensitive to BFA. Therefore, PulSA provides a very rapid method for analysis of thousands of cells following drug treatment.

Use of PulSA to sort and purify cell populations with organelle-specific markers

The use of fluorescent markers for cell sorting by flow cytometry has, to date, been restricted to differences in the intensity of the fluorescent signal on a cell-to-cell basis rather than differences associated with their intracellular location. The use of PulSA has the potential to discriminate cell populations based on differences in the location of a particular fluorescent signal.

The capacity to sort cells based on the intracellular staining pattern of a molecule would provide new opportunities to select cells with defined phenotypes. To explore this possibility we stained cell populations for three different markers, plasma membrane (Cy3-STxB), the early endosome marker EEA1 and the cis-Golgi marker GM130 and analysed by PulSA to compare the pulse-width in each population. There was a partial overlap in the fluorescent signal of each marker (Figure 5A). Significantly, PulSA showed a consistent and reproducible difference in the pulse-width of the different markers in the cell populations. EEA1-positive cells (early endosome marked cells) showed a pulse-width that was intermediate between the PM and Golgi staining patterns. To determine if cells could be sorted based on the pulse-width characteristic of each marker we mixed populations for EEA1- and GM130-stained populations (both stained with an Alexa568 conjugate) and sorted solely on the basis of the width of the fluorescent signal. Gates were established based single-labelled cell populations (Fig. 5B). From the distribution of cells in the individual gates (Fig. 5B), gate P1 represented Golgi-stained cells with very few EEA1 stained cells, gate P2 represented the overlap in pulse-width between the two populations and gate P3 with a wider pulse-width included EEA1-stained cells and only very few GM130 stained cells. Individually stained cell populations were mixed in a ratio of 1:1 and then sorted based on PulSA and cells collected from gates P1 and P3. Cells in these two gates each represented about ~10% of the total starting population. Immunofluorescence of sorted cell populations revealed that the cells from the P1 gate were cells with a tight juxtanuclear staining pattern eg. Golgi staining, whereas the cells in P3 gate were predominantly cells with a punctate staining pattern (Fig. 5B). From analyses of 100 sorted cells, 99% of cells from P1 gate had a Golgi-staining pattern while 91% of cells from P3 gate had a punctate endosomal-staining pattern. Hence, PulSA can be used to selectively enrich and purify cells based on the pulse-width of the intracellular staining pattern. Therefore, PulSA provides a rapid procedure for sorting cells based not only on a particular marker, but also on the intracellular location of the marker.

Discussion

A limitation in many studies of intracellular membrane transport is the capacity to rapidly quantitatively track the intracellular movement of cargo in a large number of individual cells within a population. The high-throughput quantitative analyses of cargo trafficking reported in this manuscript represent a significant advance for a number of applications in this field. We have shown that fluorescence pulse-width, a standard parameter of flow cytometer instrumentation, can be used to determine the location of membrane proteins, to monitor their trafficking and, in addition, can be exploited to sort cells based on differences in the intracellular localisation of membrane compartments. Our findings have the potential for pulse-width to be used for many cell biological applications. For example, pulse-width analysis of cell populations by flow cytometry can be used to monitor changes in trafficking following RNAi depletion of regulatory components, alteration in cargo trafficking as a consequence of mutations in sorting signals, and also changes in the morphology of organelles such as the Golgi.

Flow cytometry is rapid and quantitative. With flow cytometry flow rates of >10,000 cells per sec, and availability of 8-colour analyses, PulSA provides the capacity to track multiple cargos and markers within the same population simultaneously. The combination of PulSA with the power of fluorescence microscopy, to interpret the intracellular location of the different pulse widths, collectively provides information on the intracellular location of cargo in very large cell populations. In addition, flow cytometry also has the capacity to provide information on intracellular location, based on pulse-width, and also on the fluorescent intensity levels on a cell-to-cell basis. One of the complicating issues associated with transient expression of fluorescent cargo is knowledge of the level of expression and the influence of the level of expression on the transport pathway of the cargo and its intracellular location. The capacity to analyse both protein levels and the relative distribution of the protein on a cell basis within large populations should reveal complications arising from elevated levels of cargo expression. In contrast, microscopic analysis of transfected cell populations is limited in the number of cells readily analysed, does not readily provide information on total fluorescent levels within the entire cell as usually optical sections are analysed, and is subject to bias in the selection of cells for analysis.

Based on our findings, PulSA has the potential to identify mutants with altered locations. For example membrane proteins with mutations in sorting motifs required for endosome to Golgi location could be theoretically identified from large number of cells. In addition, a large number of constructs could be quickly analysed in transfected cell populations by flow cytometry to determine if there are differences in transport compared with wild-type sequences. Moreover small molecule screens which affect trafficking pathways could also be screened by flow cytometry, which would be considerable more rapid and quantitative than automated microscopy.

We also demonstrate here the capacity to sort based on intracellular location. Cells with a Golgi staining pattern were sorted with high purity from cells with an endosomal staining pattern based on pulse-width differences using the same fluorochrome for both markers. The capacity to sort cells based on differential intracellular location provides the capacity to readily isolate mutant cells with defects in trafficking. Furthermore, it is now clear that signalling can occur not only at the PM but also in intracellular compartments. The potential to separate these populations by PulSA based on the location of the activated receptor would provide a powerful approach to identify location-specific pathways associate with an activated receptor following internalisation.

The use of PulSA is particularly suited to larger cells where the difference in organelle distribution provides substantive differences in pulse-width and where the spatial discrimination between organelles is very strong. However, there is considerable potential to further optimize the system, by synchronizing cells within the cell cycle to minimize the heterogeneity in cell size, and also by improvements in instrumentation. Further, the findings presented here on retrograde

membrane transport could prompt additional applications of this technology to analyse a variety of other cell processes involving dynamic membrane events, such as apoptosis, autophagy, and mitosis.

Materials and Methods

Plasmids, antibodies and reagents

STxB was purified as described (Johannes et al., 1997) and labeled with Cy3 using an amine-reactive conjugation kit (PA23001; GE Healthcare). pcDNA–FLAG–furin, a furin construct containing the FLAG epitope tag inserted on the C-terminal end of the auto-proteolytic maturation site of the enzyme has been described previously (Chia et al., 2011). $pcDNA_3$-hWls, full-length cDNA encoding wild-type human Wntless, tagged with a HA tag at the C-terminal end and inserted into the pcDNA3 vector, was provided by Prof. Konrad Basler, University of Zurich (15). $pcDNA_3$-$hWls^{AEGL}$-HA, encoding human Wntless protein with a single site-mutation (Y425A) has been previously described (Gasnereau et al., 2011). Rabbit and mouse anti-FLAG antibodies and anti-TGN38 antibodies were purchased from Sigma Aldrich. Mouse antibodies to EEA1, LAMP1 and GM130 were from BD Biosciences (North Ryde, NSW, Australia). Mouse monoclonal antibodies to Rab9, rabbit anti-CI-MPR and rabbit anti-GRASP65 antibodies were purchased from Abcam (Cambridge, UK) and mouse monoclonal antibodies against CD63 were from Santa Cruz Biotechnology (Santa Cruz, CA). Mouse monoclonal anti-α-tubulin was obtained from GE Healthcare (Rydalmere, NSW, Australia). Secondary antibodies used for immunofluorescence were goat anti-rabbit IgG–Alexa-Fluor-568, goat anti-rabbit IgG–Alexa-Fluor-488, goat anti-mouse IgG–Alexa-Fluor-488 and goat anti-mouse IgG–Alexa-Fluor-647 were from Molecular Probes (Invitrogen, Carlsbad, CA). Horseradish-peroxidase-conjugated rabbit anti-goat Ig, horseradish-peroxidase-conjugated sheep anti-rabbit Ig and anti-mouse Ig were from DAKO Corporation (Carpinteria, CA). The siRNA against human Rab9#1 (Ganley et al., 2008) has been described previously and was purchased from Sigma Aldrich (Sydney, Australia). Brefeldin A was purchased from Sigma Aldrich (Sydney, Australia) and Can Get Signal® was purchased from Toyobo (Japan)

Cell culture and transient transfections

HeLa cells were maintained as semi-confluent monolayers in Dulbecco's modified Eagle's medium (DMEM) supplemented with 10% (v/v) fetal bovine serum (FBS), 2 mM L-glutamine, 100 U/µl penicillin and 0.1% (w/v) streptomycin (C-DMEM) in a humidified 10% CO2 atmosphere at 37°C. For transient transfections, HeLa cells were seeded as monolayers and transfected using Fugene 6 or Fugene HD (Promega, USA) according to manufacturer's instructions. Transfections were carried out in C-DMEM at 37°C, 10% CO2 for 24 hours. Transient transfections with siRNA were performed using Dharmafect 1 (Dharmacon, Thermo Scientific), according to manufacturer's instructions, for 72 hours prior to analyses.

Indirect immunofluorescence

For imaging of single cell suspensions, monolayers were lifted by incubation with 5 mM EDTA/PBS or 0.05% Trypsin/EDTA and washed twice with PBD. Cells were then fixed with 4% (w/w) paraformaldehyde (PFA) or ice-cold 10% (v/v) trichloroacetic acid (TCA) for 15 minutes, followed by quenching in 50 mM NH4Cl/PBS or 50 mM glycine/PBS respectively for 10 minutes. Cells were then permeabilised in 0.1% Triton X-100 in PBS for 4 minutes and blocked in 5% FBS in PBS for 20 minutes to reduce non-specific binding. Single cell suspensions were incubated with primary antibodies and secondary conjugates for 30 min each with washes of PBS in between. For immunolabeling of TCA-fixed samples, primary antibodies were diluted in Can Get Signal® Solution A or B (Toyobo, Japan)

Internalisation assays

For FLAG–furin trafficking assays, HeLa cells were transfected with FLAG–furin using Fugene 6 (Promega) 24 hours before the internalisation assay. For the 0 min time-point, cells were detached through incubation with 5 mM EDTA/PBS for 5 min. Suspended cells were washed with PBS and spun down, and the cell pellet was resuspended in cold diluted mouse monoclonal or rabbit polyclonal anti-FLAG antibodies (5 µg/ml) and incubated on ice for 45 min. The single cell suspension was then washed 3 times with PBS, followed by PFA fixation. For other time-points, monolayers were incubated with cold diluted FLAG antibodies for 45 min on ice, washed 3 times with cold PBS and incubated in warm SFM at 37 C for various time-points. Cells were then lifted by trypsinization and washed 2 times in cold PBS followed by PFA fixation.

For Cy3-STxB internalization assays, monolayers were incubated in Cy3-STxB diluted to 1 µg/ml in cold serum-free DMEM, and incubated on ice for 30 min. Cells were washed twice with PBS incubated at 37 ºC for various time-points in warm SFM. Cells were then lifted by trypsinization and subjected to PFA fixation. For the 0 min time-point, cells were first lifted by incubation in 5 mM EDTA/PBS, followed by washes with PBS and resuspension in cold diluted Cy3-STxB and incubation on ice. After 30 min, cells were washed 3 times in cold PBS and fixed according to the PFA fixation protocol. All FLAG-furin internalization samples were stained with fluorochrome-conjugated secondary antibodies and samples resuspended in 1 % (w/v) BSA in PBS prior to flow cytometry.

Flow cytometry and confocal microscopy

Cells were analysed at a medium flow rate in an LSRFortessa flow cytometer, equipped with 405 nm, 488 nm, 561 nm and 640 nm lasers (BD Biosciences). 50-100,000 events were collected, using a forward scatter threshold of 5,000. Data were collected in pulse height, area and width parameters for each channel. For DAPI staining, data were collected with the 405 nm laser 450/50 nm bandpass filter. For AlexaFluor 488, data were collected with the 488 nm laser 530/30 nm bandpass filter. For Cy3 and AlexaFluor 568, data were collected with the 561 nm laser and 610/20 bandpass filter.

For cell sorting, fixed single cell suspensions were sorted on a Becton Dickinson FACSAria III sorter and cells collected into eppendorf tubes. For imaging of sorted cell suspensions, . cell suspensions were pelleted onto microscope slides using a CytoSpin 4 Cytocentrifuge (Thermo Scientific), or alternatively fixed cells were dropped directly on a glass slide, followed by sealing with a coverslip and varnish. Cells were imaged with the 100×1.4 NA HCX PL APOCS oil immersion objective. Images of multicolour labelled samples were acquired sequentially. Flow cytometry data were analysed with FACSDiva software (BD Biosciences). For histogram analysis, FCS data was exported into text format using FCS Extract 1.02 software (Earl F Glynn, Stowers Institute for Medical Research) and analysed in Microsoft Prism.

Confocal optical sectioning was performed with a Leica TCS SP2 imaging system using a 100×/1.4 NA HCX PL APO CS oil immersion objective. Z-series were captured sequentially with a Z-axis step axis of 0.24 μm and 9-14 sections. Z-series were re-constructed using Leica LCS software.

Statistical analysis

Differences were assessed with the two-tailed Student's t-test using the Prism software.

Acknowledgements

We thank Dorothee Bourges for expert advice. This work was supported by funding from the Australian Research Council and National Health and Medical Research Council of Australia. PZCC was supported by a Melbourne International Graduate Scholarship.

References

1. Derby MC, Gleeson PA. New insights into membrane trafficking and protein sorting. Int Rev Cytol 2007;261:47-116.
2. Ramdzan YM, Polling S, Chia CP, Ng IH, Ormsby AR, Croft NP, Purcell AW, Bogoyevitch MA, Ng DC, Gleeson PA, Hatters DM. Tracking protein aggregation and mislocalization in cells with flow cytometry. Nat Methods 2012;9(5):467-470.
3. Wersto RP, Chrest FJ, Leary JF, Morris C, Stetler-Stevenson MA, Gabrielson E. Doublet discrimination in DNA cell-cycle analysis. Cytometry 2001;46(5):296-306.
4. Kang K, Lee SB, Yoo JH, Nho CW. Flow cytometric fluorescence pulse width analysis of etoposide-induced nuclear enlargement in HCT116 cells. Biotechnol Lett 2010;32(8):1045-1052.
5. Port F, Basler K. Wnt Trafficking: New Insights into Wnt Maturation, Secretion and Spreading. Traffic 2010.
6. Gasnereau I, Herr P, Chia PZ, Basler K, Gleeson PA. Identification of an endocytosis motif in an intracellular loop of Wntless protein, essential for its recycling and the control of Wnt protein signaling. J Biol Chem 2011;286(50):43324-43333.
7. Lieu ZZ, Gleeson PA. Endosome-to-Golgi transport pathways in physiological processes. Histol Histopathol 2011;26(3):395-408.
8. Thomas G. Furin at the cutting edge: from protein traffic to embryogenesis and disease. Nat Rev Mol Cell Biol 2002;3(10):753-766.
9. Chia PZ, Gasnereau I, Lieu ZZ, Gleeson PA. Rab9-dependent retrograde transport and endosomal sorting of the endopeptidase furin. J Cell Sci 2011;124:2403-2413.
10. Ganley IG, Espinosa E, Pfeffer SR. A syntaxin 10-SNARE complex distinguishes two distinct transport routes from endosomes to the trans-Golgi in human cells. J Cell Biol 2008;180(1):159-172.
11. Barbero P, Bittova L, Pfeffer SR. Visualization of Rab9-mediated vesicle transport from endosomes to the trans-Golgi in living cells. J Cell Biol 2002;156(3):511-518.
12. Lombardi D, Soldati T, Riederer MA, Goda Y, Zerial M, Pfeffer SR. Rab9 functions in transport between late endosomes and the trans Golgi network. Embo J 1993;12(2):677-682.
13. Riederer MA, Soldati T, Shapiro AD, Lin J, Pfeffer SR. Lysosome biogenesis requires Rab9 function and receptor recycling from endosomes to the trans-Golgi network. J Cell Biol 1994;125(3):573-582.
14. Donaldson JG, Honda A, Weigert R. Multiple activities for Arf1 at the Golgi complex. Biochimica et biophysica acta 2005;1744(3):364-373.
15. Banziger C, Soldini D, Schutt C, Zipperlen P, Hausmann G, Basler K. Wntless, a conserved membrane protein dedicated to the secretion of Wnt proteins from signaling cells. Cell 2006;125(3):509-522.

Legends to Figures

Figure 1. Pulse-width analysis of wild-type and internalization-defective Wls constructs
(A) Principle of pulse shape analysis (PulSA). Cell surface fluorescent proteins generates a wider pulse shape than intracellular fluorescent proteins with a restricted localisation. (B and C) HeLa cells were transfected with HA tagged wild-type Wls (Wls-wt) or a mutant of Wls defective in clathrin-mediated internalization Wls^{AEGL} for 48 hours. Monolayers were harvested with EDTA and cells were fixed and permeabilised and then stained for HA tagged Wls with monoclonal anti-HA antibodies (green) and for the Golgi marker, GRASP65, with rabbit anti-GRASP65 antibodies (red). (**C**) Histograms of pulse-width values are shown to provide a complete view of the dataset (n=3, mean □ SEM shown by line thickness). A statistical analysis is shown between data sets of the median pulse-width values (medium □ SEM; differences assessed by Student's t-Test). Bar represents 10 μm.

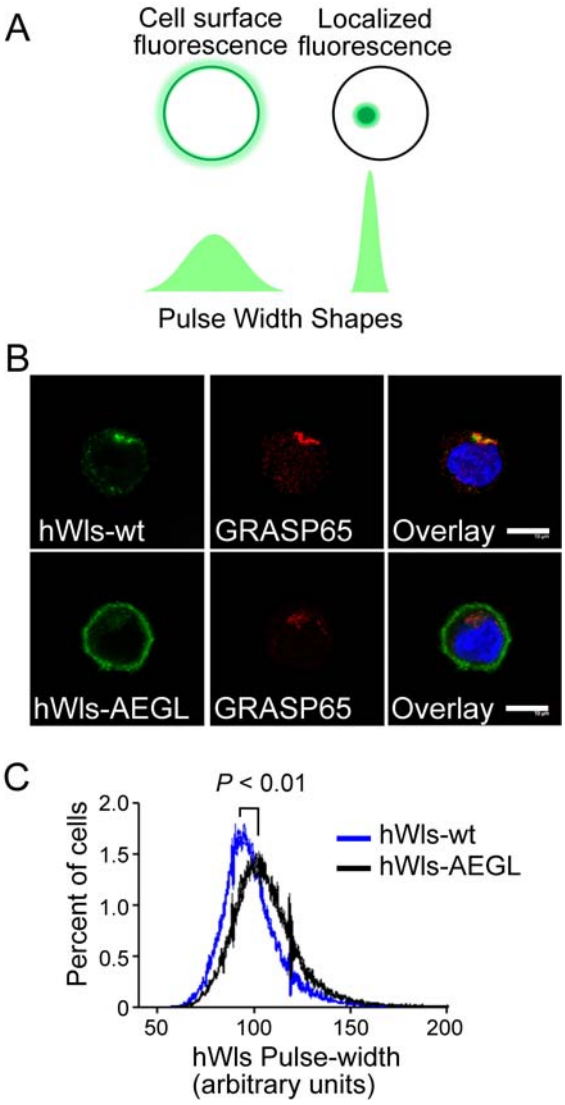

Figure 2. A flow chart for the monitoring of cargo trafficking by pulse-width analysis
Shown is the protocol for the monitoring cargo trafficking from the plasma membrane by pulse-width analysis using Shiga toxin as the example.

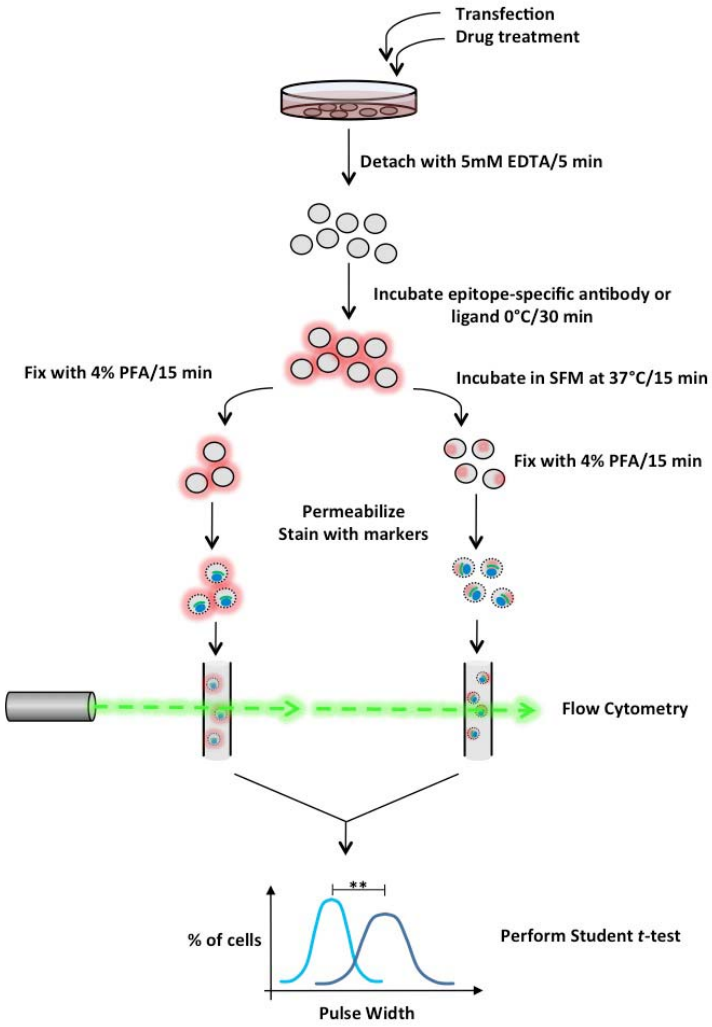

Figure 3 Monitoring the trafficking of Shiga toxin from the plasma membrane to the Golgi apparatus in cell populations by FACS.

HeLa cells in suspension were incubated Cy3-labeled STxB on ice (imaged at 0 min) and cells were incubated at 37 °C over a 30 min period. Cells were fixed, permeabilised and stained for the Golgi marker GM130 (green). (A) Pulse-width histograms of data sets for StxB and the Golgi marker, GM130, (n=3 mean □ SEM; showing different times of internalization at 37C (blue, 0 min; black, 15 min; green, 30 min). A statistical analysis is shown between data sets of the median pulse-width values (medium □ SEM; differences assessed by Student's t-Test). There was no statistical difference between the medium values of the GM130 datasets. (B) Confocal images of non-adherent HeLa cells at 0 min and 15 min internalization. Bar represents 10 μm.

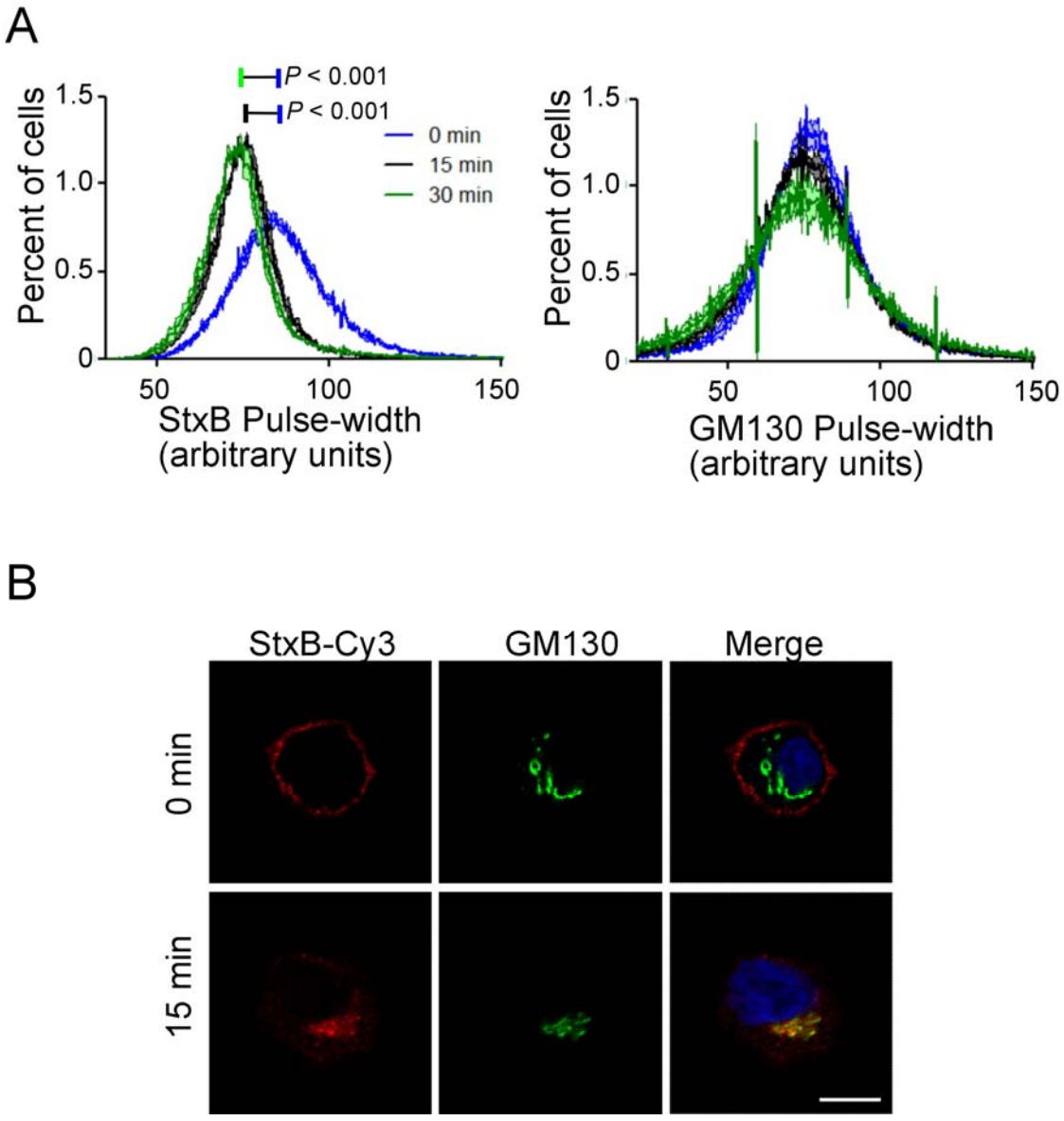

Figure 4 Monitoring effects of RNAi and Brefeldin A in cell populations by PulSA

A-B. *Effect of Rab9 silencing on intracellular location of CI-MPR*. HeLa cells were transfected with either control or Rab9 siRNA for 72 hours, monolayers either fixed or permeabilised directly or harvested and cells in suspension then fixed and permeabilised and (A) stained for Rab9 using mouse monoclonal anti-Rab9 antibodies followed by Alexa568-conjugated anti-mouse IgG. Stained adherent cells were analysed by confocal microscopy and stained cells in suspension analysed by FACS. The fluorescent intensity histograms are data sets for three independent experiments. B. RNAi-treated cells, either adherent (microscopic images) or in suspension, were stained for CI-MPR (green), the Golgi marker GRASP65 (red) and DAPI (blue). Confocal images are 3D reconstructions presented as 2D projections. Pulse-width histograms of data sets of MPR staining for control and Rab9 siRNA treated cells, (n=3 mean □ SEM). A statistical analysis is shown between data sets of the median pulse-width values (medium □ SEM; differences assessed by Student's t-Test).

(C) HeLa cells in suspension with treated with 2 ug/ml BFA or carrier alone (control) for 60 min, and the cells fixed, permeabilised and stained for GM130 (green). Pulse-width histograms of data sets for Golgi marker, GM130, (n=3 mean □SEM). A statistical analysis is shown between data sets of the median pulse-width values (medium □ SEM; differences assessed by Student's t-Test). Microscopic images are 3D reconstructions, presented as 2D projections, of cytospin-collected stained cells; GM130, green; DAP1, blue. Bar represents 10 μm.

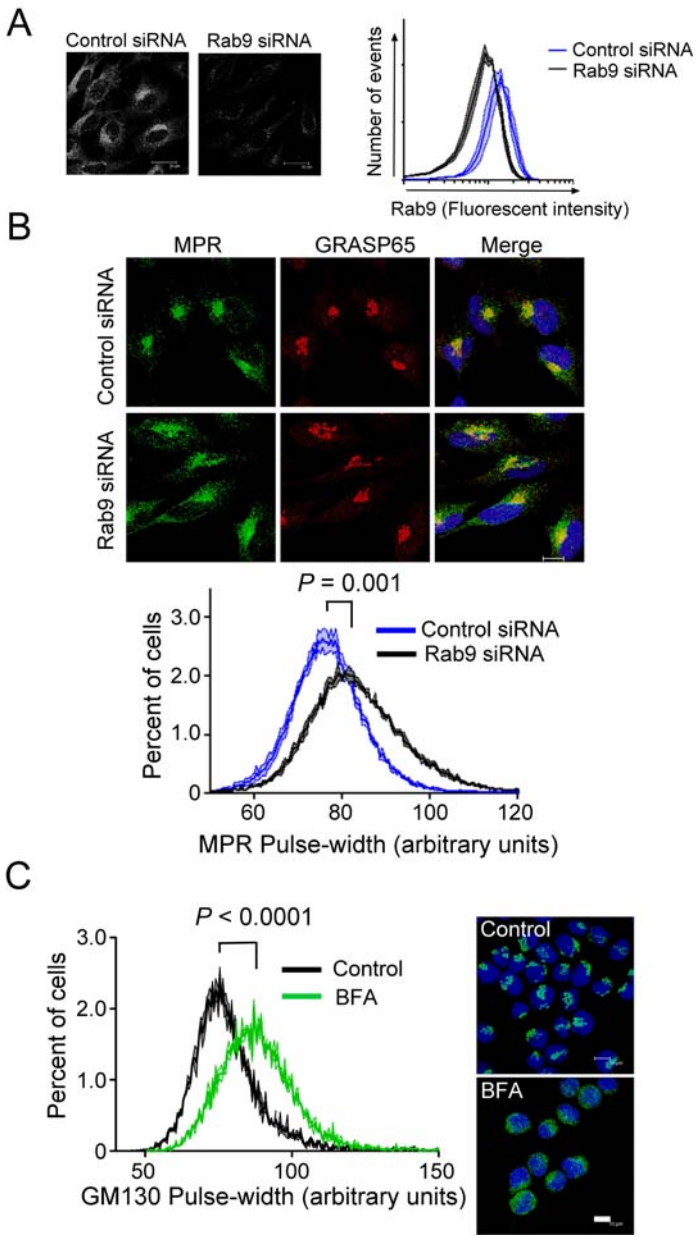

Figure 5 Cell sorting using pulse-width to distinguish differences in intracellular location

A. Pulse-width histograms of suspension cultured HeLa cells stained for either plasma membrane with Cy3-STxB for 30 min on ice then the cells fixed, or the cell suspension fixed and permeabilised and stained for the endosome marker EEA1 or the cis-Golgi marker GM130 with the relevant monoclonal antibodies followed by Alexa568-conjugated anti-mouse IgG (red).

B. Suspension cultured HeLa cells were fixed, permeabilised and stained with either monoclonal anti-GM130 or monoclonal anti-EEA1 antibodies followed Alexa568-conjugated anti-mouse IgG (red). 3D reconstructions shown. FACS anaysis of each population showing dot plot of forward scatter (Y axis) and Pulse-with (Alexa568). Gates are indicated, P1, P2, P3 for individual populations and a 50/50 mix of the two populations. Bottom: Confocal images of sorted cells from P1 and P3 gates. Shown are 3D reconstructions presented as 2D projections. Bars represent 10 μm.